A DENSITY FUNCTIONAL THEORY (DFT) STUDY ON SILICON DOPED CARBON NANOTUBE Si-CNT AS A CARRIER FOR BMSF-BENZ DRUG USED FOR OSTEOPOROSIS DISEASE

TEORÍA DEL FUNCIONAL DE LA DENSIDAD (DFT) SOBRE NANOTUBOS DE CARBONO DOPADOS CON SILICIO Si-CNT COMO PORTADOR DEL FÁRMACO BMSF-BENZ UTILIZADO PARA LA ENFERMEDAD DE OSTEOPOROSIS

Zaid H. Al-Sawaff[1,2], Serap Senturk Dalgic[3], Fatma Kandemirli[4]

[1] Material Science & Engineering Dept., Faculty of Engineering and Architecture, Kastamonu University, Turkey.
[2] Medical Instrumentation Technology, Technical Engineering College, Northern Technical University, Mosul, Iraq.
[3] Department of Physics, Faculty of Science, Trakya University, 22030, Edirne, Turkey.
[4] Biomedical Engineering Department, Faculty of Engineering & Architecture, Kastamonu University, Kastamonu, Turkey.

(Recibido: 10/2021. Aceptado: 01/2022)

Abstract

This study aims to investigate the capability of Silicon-Doped Carbon Nanotube (Si-CNT) to detect and adsorb the BMSF-BENZ ((4-Bromo-7-methoxy-1-(2-methoxyethyl)-5-{ [3-(methylsulfonyl)phenyl] methyl } - 2 - [4 - (propane-2-))yl) phenyl] - 1H - 1, 3-benzothiazole) molecular. For this purpose, we considered different configurations for adsorbing BMSF-BENZ drugs on the surface of the Si-CNT nanotube. All considered configurations are optimized using the density functional theory (DFT) at the 6-31G** basis set and B3LYP-B97D level of theory. Then from optimized structures, for each nanoparticle, we selected seven stable locations for the adsorption of BMSF-BENZ in (Br, N_8, N_9, N_{58}, O_{35}, O_{41} and S) active atoms on the surface of the selected nanoparticle. The quantum theory of atoms in molecules

Zaid H. Al-Sawaff: zaidalsawaff@ntu.edu.iq https://doi.org/10.15446/mo.n64.99010

(QTAIM), reduced density gradient (RDG) analysis, and molecular orbital (MO) analysis were also established. The calculated results indicate that the distance between nanotube and drug from the N_8 site is lower than from all other locations sites for all investigated complexes, and adsorption of BMSF-BENZ from the N_8 site is more favorable for the Si-CNT nanotube. The adsorption energy, hardness, softness, and fermi energy results reveal that the interaction of BMSF-BENZ with Si-CNT is a promising adsorbent for this drug as Adsorption energy Eads of BMSF-BENZ/Si-CNT complexes are (-13.08, -43.50, -17.90, -31.29, -25.57, -16.56, and -28.05) kcal/mol in the gas phase. As well, the appropriate and spontaneous interaction between the BMSF-BENZ drug and Si-CNT nanoparticle was confirmed by investigating the quantum chemical molecular descriptors and solvation Gibbs free energies of all atoms.

Keywords: BMSF-BENZ; drug adsorption; drug delivery system; density functional theory; thermodynamic properties.

Resumen

Este estudio tiene como objetivo investigar la capacidad de los nanotubos de carbono dopados con silicio (Si-CNT) para detectar y adsorber el BMSF-BENZ ((4 -Bromo -7 -metoxi -1 -(2 - metoxietil)-5 -{ [3-(metilsulfonil) fenil]metil } - 2 - [4 - (propano-2-))il) fenil] - 1H - 1, 3-benzotiazol) molecular. Para ello, consideramos diferentes configuraciones para adsorber fármacos BMSF-BENZ en la superficie del nanotubo Si-CNT. Todas las configuraciones consideradas se optimizan utilizando la teoría del funcional de la densidad (DFT) en el conjunto básico 6-31G** y los niveles de teoría B3LYP-B97D. Luego, a partir de estructuras optimizadas para cada nanopartícula, seleccionamos siete ubicaciones estables para la adsorción de BMSF-BENZ en (Br, N_8, N_9, N_{58}, O_{35}, O_{41} y S) átomos activos en la superficie de la nanopartícula seleccionada. También se establecieron la teoría cuántica de átomos en moléculas (QTAIM), el análisis de gradiente de densidad reducida (RDG) y el análisis orbital molecular (MO). Los resultados calculados

indican que la distancia entre el nanotubo y el fármaco desde el sitio N_8 es menor que desde todos los demás sitios de ubicación para todos los complejos investigados y la adsorción de BMSF-BENZ desde el sitio N_8 es más favorable para el nanotubo Si-CNT. Los resultados de energía de adsorción, dureza, suavidad y energía de Fermi revelan que la interacción de BMSF-BENZ con Si-CNT es un adsorbente prometedor para este fármaco, ya que los Eads de energía de adsorción de los complejos BMSF-BENZ/Si-CNT son (-13.08, - 43.50, -17.90, -31.29, -25.57, -16.56, y -28.05) kcal/mol en la fase gaseosa. Además, la interacción adecuada y espontánea entre el fármaco BMSF-BENZ y la nanopartícula Si-CNT se confirmó investigando los descriptores moleculares químicos cuánticos y las energías libres de Gibbs de solvatación de todos los átomos.

Palabras clave: BMSF-BENZ; adsorción de fármacos; sistema de administración de fármacos; teoría funcional de la densidad; propiedades termodinámicas.

Introduction

Based on its appropriate and practically validated chemical and physical properties [1–4], one of the BMSF-BENZ derivatives used in the treatment of osteoporosis was selected in our article. The most important properties of this compound with the chemical structure ((4 -Bromo -7 -methoxy -1 -(2- methoxyethyl) - 5 -{ [3 -(methylsulfonyl) phenyl]methyl}-2-[4-(propane-2-))yl) phenyl] -1H-1,3-benzothiazole) (Figure 1) is its ability to exhibit peak releasing hormone (PTH) and novel properties concerning the CaSR receptor [4].

With the growing development of nanoscience, the facts of nanostructures like nanosheets, nanocomposites, nanotubes, and nano cells were extensively studied as possible candidates in many different fields [5–9]. Nanotubes are best suited as drug carriers because of their high sensitivity to drug molecules, low side effects, unique surface properties, atomic structures, etc. [10–12].

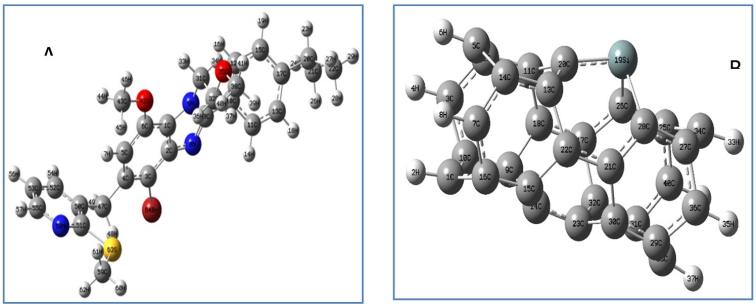

FIGURE 1. *Optimized structures of isolated molecular fragments, and B segments of SWCNTs obtained using B97D/6-31G** (d) in the gas phase.*

In 2012, Sazan M. Haidary *et al.* introduced a review on Nanoporous Silicon as Drug Delivery Systems for Cancer Therapies, and they showed that porous silicon nanoparticles (PSi) had been established as excellent candidates for medical applications as drug delivery devices due to their excellent biocompatibility, biodegradability, and high surface area [13].

Moreover, in 2013, PA Gowri Sankar and Udhayakumar Kaithamalai conducted a comparative DFT study on the electronic properties of the zigzag boron silicon (10,0) single-walled carbon nanotubes on gas molecular adsorption using nine dominant gas molecules (H_2, H_2O, O_2, CO, CO_2, NO, NO_2, NH_3, and CH_3OH) to exploit their potential applications as gas sensors [14]. They found that all molecules are weakly adsorbed on the original carbon nanotube adsorbent with small binding energy, while they can be either charge donors or acceptors of the nanotubes. Also, they showed that the adsorbents B-CNT and Si-CNT were highly chemicals when they were exposed to NO, NO_2, O_2, and CH_3OH.

F.J. Martínez-Vázquez *et al.* published an article in 2013 dealing with the fabrication of novel Si-doped Hydroxyapatite/Gelatine scaffolds at room temperature by fast prototyping for drug delivery system and bone regeneration, and they proved that the scaffold behaves as a hydrogel palliative the fitting to the bone defect at the time of surgery. These scaffolds show a sufficient macropore design for vascularization and a microporosity that enables fluid

exchange, and the compressive conduct of such scaffolds is similar to that of trabecular bone of the same density. Moreover, *In vitro* cellular investigations acquired in the well-established osteoblastic cell line MC_3T_3-E1 exposed various benefits of gelatin inclusion in the material regarding cell differentiation and gene expression. Finally, the investigation indicated that these composite scaffolds are sufficient to be considered as matrices for bone regeneration and drug delivery [15].

In 2018, Rayeheh Bagheri *et al.* introduced a DFT study about Si-doped phagraphene as a drug carrier for Adrucil anti-cancer drugs [16]. Based on the results, the Adrucil drug interacts very weakly with phagraphene. However, after replacing one carbon atom with different atoms like Al, Si, and B, the results showed that the new complex of drug/Si-CNT is more appropriate for Adrucil delivery because of moderate adsorption energy, short recovery time, and the electronically harmless adsorption property [16]. No previous investigation of BMSF-BENZ adsorption on Si-CNT(4,0) has been performed to the authors' knowledge.

The main objective of this research is to investigate the adsorption behavior of BMSF-BENZ on the zigzag surface of Si-CNT(4,0)SWCNT. For this purpose, we have conducted a comparative investigation of various structural and electronic properties before and after the adsorption of BMSF-BENZ onto the nanotube.

Computational methods

All calculations were performed using density functional theory (DFT) based on 6-31G** as a basis set and B3LYP-B97D level of theory due to its accuracy [17–20], using Gaussian 09 package [21]. In this work, the vibrational frequencies of all the new complexes with the original compounds were analyzed and examined to verify the actual global minimum for the predicted Si-CNT nanotubes. The adsorption energy, energy gap change, charge transfer analysis, dipole moment, and recovery time were also investigated to predict the interaction of drug molecules with nanoparticles.

In order to obtain the electrical properties of the complexes, the E_{HOMO} and E_{LUMO} energies correspond to the highest occupied molecular orbital (HOMO) and lowest occupied molecular orbital (LUMO), respectively. Also, some physical and chemical parameters based on E_{HOMO} and E_{LUMO} energies, such as electronegativity (χ), Fermi energy level (E_f), and energy gap (for example), can be calculated by the following equations: [22–25]

$$\chi = -\frac{1}{2}(E_{HOMO} + E_{LUMO}) \tag{1}$$

$$E_f = E_{HOMO} + \frac{(E_{LUMO} - E_{HOMO})}{2} = -\chi \tag{2}$$

$$E_g = E_{LUMO} - E_{HOMO} \tag{3}$$

Several calculations were executed to calculate the total energies of the molecules depending on the position of the nanotube attached to the drug molecule. The adsorption energies of drug on the surfaces of the nanotubes were obtained by: [26]

$$E_{ads} = E_{complex} - (E_{nanotube} + E_{drug}) \tag{4}$$

where $E_{complex}$, $E_{nanotube}$ and E_{drug} donate the energy of the complex composed with nanotubes–drug and isolated energies of nanotube and drug, respectively. The E_{ads} energy was determined from the summation of the interaction energy (E_{int}) and deformation energies (E_{def}) of the drug ($E_{def-drug}$) and nanotubes (E_{def} - $_{nanotube}$) during the adsorption process. [27]

$$E_{int} = E_{complex} - (E_{nanotube\ in\ complex} + E_{drug\ in\ complex}) \tag{5}$$

$$E_{def} = (E_{drug\ in\ complex} - E_{drug}) + (E_{nanotube\ in\ complex} - E_{nanotube}) \tag{6}$$

where $E_{nanotube\ in\ complex}$, $E_{drug\ in\ complex}$ are the energies of nanotube and drug with their geometries in the complex, respectively.

The thermodynamical parameters were also investigated such as changing in Gibbs free energy (ΔG), entropy (ΔS), and enthalpy (ΔH), to examine the structural stability using the following equations: [28]

$$\Delta G = G_{complex} - G_{nanotube} - G_{drug} \tag{7}$$

$$\Delta H = H_{complex} - H_{nanotube} - H_{drug} \tag{8}$$

$$\Delta S = \frac{\Delta H - \Delta G}{T} \tag{9}$$

where $G_{complex}$ and $H_{complex}$ are the Gibbs free energy and the enthalpy of drug adsorbed upon nanotubes, G_{nano} and H_{nano} are the Gibbs free energy and enthalpy of the nanotubes, and G_{drug} and H_{drug} are the Gibbs free energy and enthalpy of the drug, respectively. (T) is the room temperature equal to (298.15K).

The nature of interactions between BMSF-BENZ and Si-CNT has been determined by the quantum theory of atoms in molecules (QTAIM) analysis of Bader's, [29] which is implemented in Multiwfn program [30]. The non-covalent interaction (NCI) analysis was obtained through Multiwfn 3.7 program by the reduced density gradient (RDG) of quantum mechanical electron density. The RDG scatter plots versus the second largest eigenvalue of the Hessian matrix of electron density were created by Multiwfn 3.7 program [30]. The coloured maps of scatter points were plotted by gnu-plot 5.7 program [31]. The molecular orbital (MO) analysis has been evaluated by Multiwfn 3.7 program using the density of states (DOS). Recovery time has been predicted to understand the desorption process of the drug molecule from the Si-CNT surface when the adsorbent is in the gas phase.

Results and discussions

The optimized geometry of the adsorbents

An adsorbent nanotube of zigzag Si-doped SWCNT (n,0) was used on the BMSF-BENZ drug as an osteoporosis disease drug delivery

vehicle. The nanotube and BMSF-BENZ molecule were initially optimized using DFT calculation in the gas phase. The optimized geometries of adsorbent Si-CNT and drug molecules with their corresponding HOMO, LUMO, are shown in Figure 2.

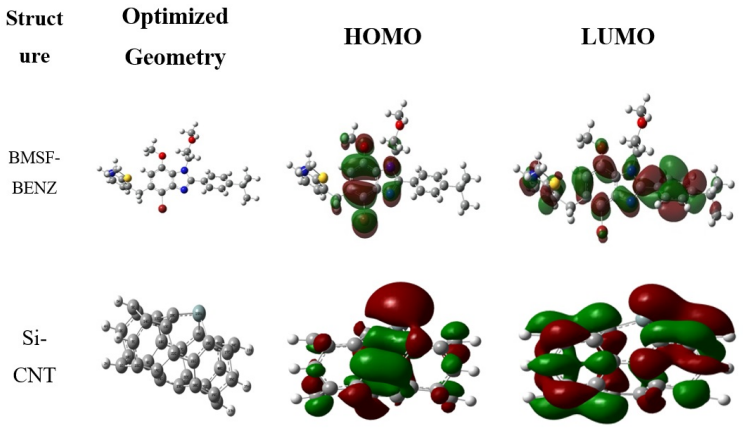

FIGURE 2. *Structures, HOMO, LUMO for the BMSF-BENZ drug, Si-CNT using B97D/6-31G** (d) in the gas phase.*

The vibrational modes for the new complexes and the original compounds were calculated to check the structural stability in the presence of IR. Where all compounds give vibrational modes with a positive frequency range of ((-186.92, -195.46, -197.16, -205.89, -201.41, -188.75, and -244.98) cm^{-1} as a minimum value, and (3215.99, 3224.04, 3205.05, 3216.90, 3214.86, 3218.96, 3208.32) cm^{-1} as a maximum value for the active atom binding (Br, N_8, N_9, N_{58}, O_{35}, O_{41}, and S) with Si-CNT nanotube (Figure 3). Furthermore, the HOMO and LUMO energies were also calculated to find the energy gap of nanotubes.

HOMO levels are located on the center of the C–C bonds throughout the nanotube, whereas LUMO levels were located all over the nanotube structure. The predicted energy gap of Si-CNT (0,62, 0,59, 0,60, 0,48, 0,69, 0,60, and 0,68) eV for all locations, respectively.

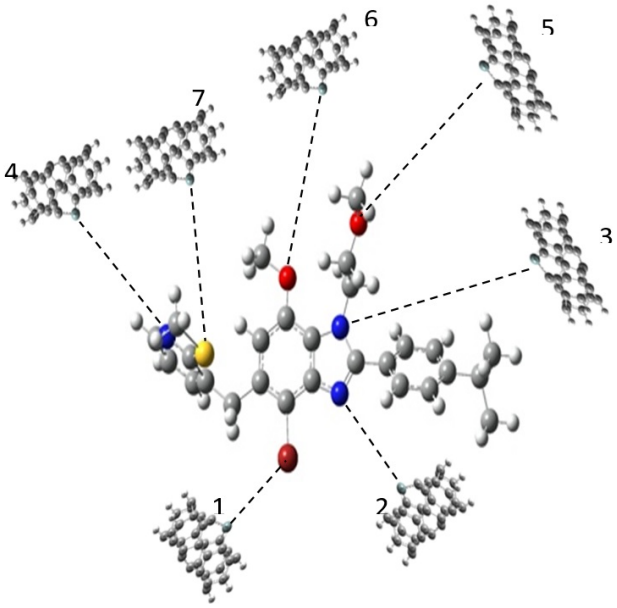

FIGURE 3. *Location of the active atoms of BMSF-BENZ where Si-doped CNT was interacting: (1) Bromine atom, (2) Nitrogen N_8 atom, (3) Nitrogen N_9 atom, (4) Nitrogen N_{58} atom, (5) Oxygen O_{35} atom, (6) Oxygen O_{41} atom, and (7) Sulfur S atom.*

BMSF-BENZ adsorption on Si-CNT nanotube

To detect suitable adsorbents for BMSF-BENZ, we attempted to verify various properties like geometric, electronic, adsorption properties, etc., of BMSF-BENZ/Si-CNT complexes. Initially, Si-CNT was exposed to the drug compound at different adsorption sites and the preferred adsorption sites for Si atoms were found as it approached (Br, N_8, N_9, N_{58}, O_{35}, O_{41}, S) atoms of BMSF-Benz (Figure 3).

In the case of the BMSF-BENZ adsorbed compound, the Si-CNT geometry remains unchanged, and the lengths of the C-C bonds varied by about 0.03 $\AA$ at the proximal adsorption site. It claims that there is an interaction between BMSF-BENZ and Si-CNT nanotubes, and this was confirmed by the adsorption energy and changes in the electronic properties analysis except when the

nanotube approached the N_9 nitrogen atom. We observed that the bond length was the same before and after adsorption, which means that there is no interaction between the nanotube and the drug compound at this point.

The BMSF-BENZ drug molecule was adsorbed on the Si-CNT nanotube with an adsorption energy of about (-13.08, -43.50, -17.90, -31.29, -25.57, -16.56 and -28,05) kcal/mol at a distance of at least about (3.27, 1.91, 8.32, 1.94, 1.90, 3.91, and 2.37) $\mathring{A}$ in the B3LYP-B97D method as shown in Table 1.

Due to the proximity of the bromine atom to the interaction region between the nanoparticle and the nitrogen atom (N_9), the bromine atom forced the silicon atom to move away from the nitrogen atom and prevented it from forming a bond between them, but instead, hydrogen bonds were formed between two hydrogen atoms in the nanoparticle with an atom Nitrogen in the drug compound and with spaces (1.91, 1.85) $\mathring{A}$ respectively.

In order to analyze the adsorption and desorption process together, the charge Q(e) values for Si-CNT by adsorption process and recovery time were obtained Under vacuum UV light conditions with a frequency of (3×10^{16}) sec^{-1} at room temperature for the different complexes in the gas phase shown in Table 1.

Note that the length of the bonds between the silicon atom and the adjacent carbon atoms were (1.80, 1.89, 1.89) $\mathring{A}$, respectively, and the distance between the Si-CNT and every active atoms was (2.4) $\mathring{A}$.

Dipole moment refers to the polarity of the compound as it appears due to the asymmetric charge distribution as well as the difference in electronegativity between the resultant molecules or atoms, where the large dipole moment refers to the more polar structure which results in a more stable interaction of the structure [32].

The results of the dipole moment showed that the new compounds obtained from the adsorption of the drug compound on the surface of the nanotube had different values greater than the value that the drug had before adsorption. A more stable reaction occurred when the drug compound was adsorbed on the surface of the nanotube

Structure	d	E_{ads}	E_{int}	E_{def}	Bond location	Bond length after adsorption	DM	τ (sec)
BMSF-BENZ	-	-	-	-	-	-	1.82	-
Si-CNT	-	-	-	-	-	-	0.64	-
					Si-C1	1.79		
Br/Si-CNT	3.27	-13.08	307,13	-320,20	Si-C2	1.88	2.20	2.39×10^{15}
					Si-C3	1.88		
					Si-C1	1.79		
N_8/Si-CNT	1.91	-43.50	266,30	-309,80	Si-C2	1.85	5.92	4.27×10^{-4}
					Si-C3	1.86		
					Si-C1	1.80		
N_9/Si-CNT	8.32	-17.90	-325,41	307,51	Si-C2	1.89	1.70	2762059
					Si-C3	1.89		
					Si-C1	1.79		
N_{58}/Si-CNT	1.94	-31.29	276.85	-308.14	Si-C2	1.84	3.02	177.49
					Si-C3	1.89		
					Si-C1	1.78		
O_{35}/Si-CNT	1.90	-25.57	284.46	-310.03	Si-C2	1.84	1.63	4.49×10^{-05}
					Si-C3	1.84		
					Si-C1	1.79		
O_{41}/Si-CNT	3.91	-16.56	257.82	-274.38	Si-C2	1.88	0.71	11537.95
					Si-C3	1.88		
					Si-C1	1.78		
S/Si-CNT	2.37	-28.05	-237.84	237.80	Si-C2	1.84	1.94	3.33×10^{-17}
					Si-C3	1.84		

TABLE 1. *Adsorption energy (E_{ads}), Interaction energy (E_{int}), and deformation energies (E_{def}) in (kcal/mol), the distance between BMSF-BENZ molecule, and adsorbents (d) in (Å), bond length between active atoms of the nanotubes after adsorption of BMSF-BENZ drug for the different complex in gas phase, the DM denotes the dipole moment values of Si-CNT in (Debye) and recovery time (τ) in sec.*

at N_8 atom with the value of (5.92) Debye, which was greater than the rest of the other active atoms of the drug compound.

The Quantum Theory of Atom in Molecule (QTAIM) Analysis

In order to understand the nature of interactions of BMSF-BENZ drug on Si-CNTs, topology analysis based on Bader's QTAIM method has been employed with Multiwfn program. The QTAIM

theory is one of the most powerful methods to investigate the nature of intermolecular interactions. This theory explains the concepts of chemical bond between components and supplies the exact information on the electronic structure.

In QTAIM analysis, the nature of intermolecular interactions between drug and Si-CNT is determined in terms of electron densities at bond critical points (BCPs).

The electron density of $\rho(r)$ and laplacian $\nabla^2\rho(r)$ characteristics are widely used to understand the bonding interactions nature. However, the other two parameters of total energy density of H(r) and the ratio of $|V(r)|/G(r)$ are more remarkable parameters used on bonding characteristics. The covalent bonding characteristics correspond to $\nabla^2\rho(r) < 0, H(r) < 0, |V(r)|/(G(r) > 2)$. The strong hydrogen bonds as the intermediate type of interaction related to $\nabla^2\rho(r) > 0, H(r) < 0, 1 < |V(r)|)/(G(r) < 2)$. The weak and medium-strength hydrogen bonding and Van der Waals interactions due to the $\nabla^2\rho(r) > 0, H(r) > 0, |V(r)|/G(r) < 1$.

In this work, the QTAIM theory has been applied for the N_8/Si-CNT, N_{58}/Si-CNT and O_{35}/Si-CNT complexes which appeared having the higher adsorption energy values (in magnitude) given in Table 1. The calculated QTAIM parameters at B3LYP-B97D level of theory are displayed in Table 2. The interactions between the drug and Si-CNT for the selected complexes are shown in Figure 4.

It is clear in Table 2 the nature of interactions between Si-CNT nanotube and N_{41} site, Si_{19} site and O_{35} site atoms are partial-covalent character with the ratio of $|V_{BCP}|/G_{BCP} > 1$, which are calculated at both B3LYP-B97D level of theory. Those interactions can be classified as the intermediate type of interaction with $(\nabla^2\rho_{BCP} > 0)$ with $(H_{BCP} < 0)$ rule.

All remaining interactions in Table 2 exhibit mainly van der Waals type weak and with medium-strength hydrogen bonding due to the ratio of $|V_{BCP}|/G_{BCP} < 1$.

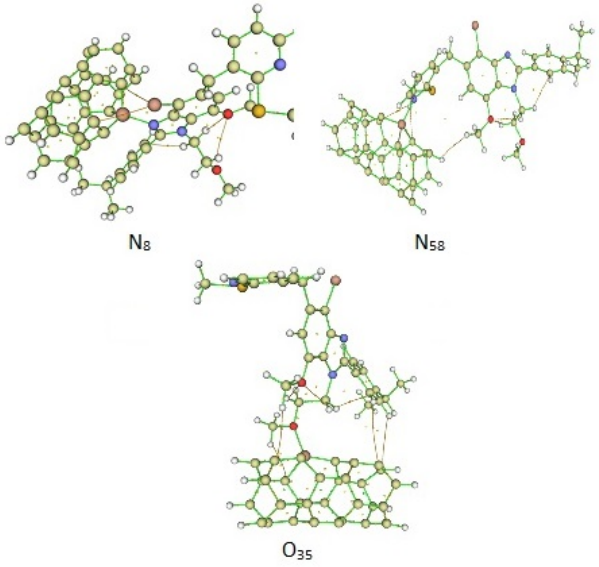

FIGURE 4. *The computed molecular topographical map of the complexes for BMSF-N_8/Si-CNT, BMSF-N_{58}/Si-CNT, and BMSF-N_{58}/Si-CNT. The bond critical points are represented by orange spheres. The ring and cage critical points are displayed with yellow and green circles. The lines are bond paths.*

Stru.	BCPs Drug/CNT	ρ_{BCP}	$\nabla^2\rho_{BCP}$	G_{BCP}	V_{BCP}	H_{BCP}	$\lvert V_{BCP}\rvert/G_{BCP}$
N_8/CNT	N_{41}-Si_{19}	0.0823335	0.2941107	0.1018591	-0.1301905	-0.0283314	1.2781432
	Br_{50}-C_{26}	0.0125550	0.0366143	0.0074981	-0.0058427	0.0016554	0.7792241
	Br_{50}-C_{11}	0.0073456	0.0208577	0.0041870	-0.0031596	0.0010274	0.7546214
	N_{41}-Si_{19}	0.0796940	0.2454279	0.0911090	-0.1208611	-0.0297520	1.3265550
N_{58}/CNT	H_{57}-C_{11}	0.0071698	0.0244838	0.0047799	-0.0034388	0.0013411	0.7194292
	H_{57}-C_{26}	0.0092348	0.0310669	0.0061763	-0.0045859	0.0015904	0.7424995
	H_{74}-H_{33}	0.0038879	0.0136617	0.0024959	-0.0015763	0.91956×10^{-03}	0.6315551
	H_{75}-C_{25}	0.0028796	0.0082285	0.0015306	-0.0010040	-0.2022543	0.6559519
O_{35}/CNT	O_{41}-Si_{19}	0.0695024	0.2791836	0.0878699	-0.1059439	-0.0180739	1.2056904
	H_{49}-C_{28}	0.0117055	0.0402081	0.0082100	-0.0063681	0.0018419	0.7756511
	H_{71}-C_{12}	0.0012479	0.0040831	0.0007309	-0.0004410	0.0002899	0.6033652
	H_{78}-C_5	0.0013651	0.0042071	0.0007931	-0.0005345	0.0002586	0.6739377

TABLE 2. *The QTAIM parameters of selected complexes at the BCPs. Electron density ($\rho(r)$), Laplacian of electron density ($\nabla^2\rho(r)$), the kinetic electron density (G(r)), potential electron density (V(r)), total electron energy density (H(r)), the ratio $|V_{BCP}|/G_{BCP}$.*

RDG Analysis

To understand the non-covalent interactions between BMSF-BENZ drug and Si-CNT, the RDG is calculated by Multiwfn using the following definition as

$$RDG(r) = \frac{1}{2(3\pi^2)^{\frac{1}{3}}} \frac{|\Delta\rho(r)|}{\rho(r)^{\frac{4}{3}}} \tag{10}$$

where ρ is electron density and r is coordinate vector. The $\rho(r)$ values obtain the strength of bonds, and the function with sign (λ_2), where λ_2 is referred the second largest eigenvalue of the Hessian matrix of $\rho(r)$. The colour mapped scatter plots of RDG versus $(\text{sign}\lambda_2)\rho$ for the selected complexes of N_8 and N_{58} site atom given in Table 2 are drawn by Gnu-plot and shown in Figure 5, by comparison with those obtained for Si-CNT one. In this scatter plot, the red, green and blue color indicate the strong repulsive interactions ($\rho < 0$ and $\lambda_2 > 0$, relate to repulsion forces and steric effect), van der Walls interactions (ρ=0 and λ_2=0) and strong attraction ($\rho > 0$ and $\lambda_2 < 0$, relate to electrostatic, hydrogen bonding), respectively. As shown in Figure 5, most RDG density is localized at around $\lambda_2 = 0$ and $\lambda_2 < 0$ regions; thereby, it is pointed out that the interactions between BMSF-BENZ drug and Si-CNT in the presented complexes are predominantly non-covalent and van der Walls type. This finding is consistent with the QTAIM results. Comparison results in Figure 5 that the RDG scatter in N_8 and N_9 atom site complexes in the $\lambda_2 = 0$ and $\lambda_2 < 0$ regions are distributed larger area than in Figure 5a for Si-CNT. The RDG scatter points in the van der Walls region takes on an almost identical shape with B3LYP-B97D method.

The quantum descriptors denoted by Equations (1- 4) are calculated for BMSF-BENZ/Si-CNT complex structures and given in Table 3. In the BMSF-BENZ/Si-CNT structure, the electronic parameters such as E_{HOMO}, E_{LUMO}, Eg, and Fermi energies have a noticeable change. The values of E_{HOMO} and E_{LUMO} of Si-CNT nanotubes before the adsorption of molecules are (-4.35 and -3.77) eV, and after adsorption of BMSF-BENZ drug are mentioned in

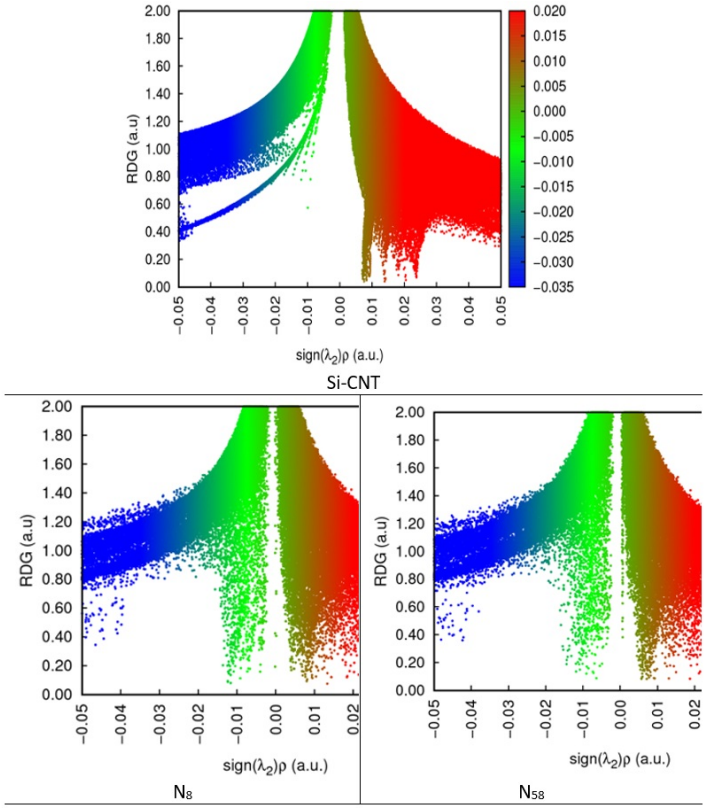

FIGURE 5. *RDG plots BMSF-BENZ adsorption from N_8 and N_{59} site on the surface of Si doped CNT at the B97D level of theory. The scatter graphs calculated by 6-31** basis set and B3LYP-B97D methods.*

Table 3. The sensors are related to the variation of their electrical conductance after drug adsorption due to the electron exchange between the drug and sensor. On this line, the CNT sensitivity to the drug is based on the changing of HOMO and LUMO energies with E_g.

In order to understand the sensing mechanism of the Si-CNT to drug, the percentage variation of $\%\Delta E_g$ energy gap during the adsorption process is taken into account by the following equation:

$$\%\Delta E_g = 100x(E_{g2} - E_{g1})/E_{g1} \tag{11}$$

where E_{g1} and E_{g2} are the E_g values of CNT and complex structure, respectively. The percentage change values, of $\%\Delta Eg$ for each structure are given in Table 3. The percent change in the work function as $\%\Delta\Phi$ can be derived by logic in band gap energies given in Eq. (9).

The corresponding frontier molecular orbital map is shown in Figure 6, and the Frontier molecular orbital (HOMO and LUMO) of all investigated complexes is shown in Figure 7. Thus, the BMSF-BENZ drug molecule was significantly affecting the HOMO energy level and LUMO energy level as shown in Table 3.

Structure	$\mathbf{E}_{HOMO}$ **(eV)**	$\mathbf{E}_{LUMO}$ **(eV)**	$\mathbf{E}_g$	$\%\Delta E_g$	**Ef (eV)**	Φ	$\%\Delta\Phi$
BMSF-BENZ	-4.57	-1.43	3.14	-	-3.00	3.00	-
Si-CNT	-4.36	-3.78	0.58	-	-4.07	4.07	-
Br/Si-CNT	-4.05	-3.43	0.62	7.67	-3.74	3.74	8.08
N_8/Si-CNT	-2.98	-2.39	0.59	2.68	-2.69	2.69	33.97
N_9/Si-CNT	-4.01	-3.41	0.60	4.10	-3.71	3.71	8.78
N_{58}/Si-CNT	-3.51	-3.02	0.48	16.15	-3.27	3.27	19.68
O_{35}/Si-CNT	-3.68	-2.99	0.69	19.73	-3.34	3.34	17.98
O_{41}/Si-CNT	-4.39	-3.78	0.61	5.08	-4.09	4.09	0.44
S/Si-CNT	-3.59	-2.90	0.69	19.07	-3.29	3.29	20.20

TABLE 3. *Calculated E_{HOMO}, E_{LUMO} energies, HOMO-LUMO gap (E_g), Fermi level energy (E_f), and work function (Φ), the percentage variation of E_g and Φ respect to bare Si-CNT for the studied complexes.*

As reported energies of E_{HOMO}, E_{LUMO} and E_g in Table 3, some electronic properties of Si-CNT are affected weakly by the adsorption of the BMSF-BENZ drug. The decreasing order of percentage change values are obtained for the interactions of N_8, and N_{58} atoms of the BMSF-BENZ drug with Si-CNT.

It is known that the lower E_g values indicate higher electrical conductivity, reactivity, and sensitivity. Therefore, decreasing the E_g through adsorption of the BMSF-BENZ drug molecule indicates that the Si-CNT can detect the drug. Thus, among all studied

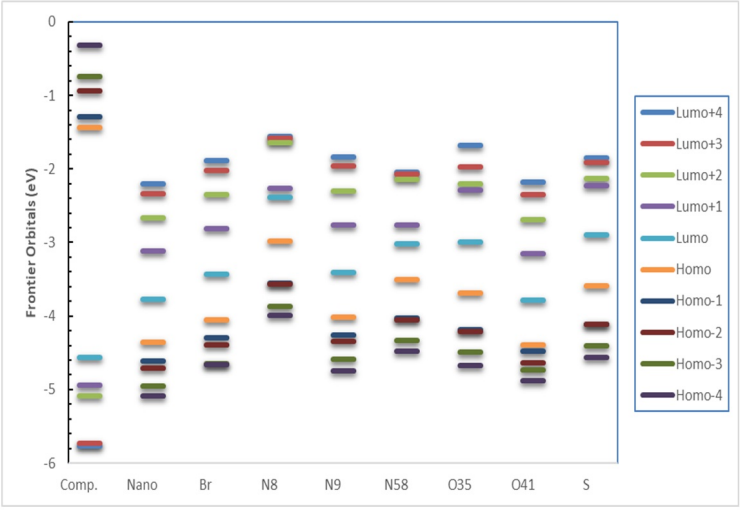

FIGURE 6. *Energy gap between HOMO and LUMO for BMSF-BENZ drug, Si-CNT nanotube for all investigated locations regarding to the position of the nanotube on the drug using 6-31** basis set with B3LYP-B97D level of theory.*

geometries of complex structures, the highest variation value of $\%E_g$ has been obtained by the N_{58} atom of the BMSF-BENZ interacts with Si-CNT nanotube. According to the values of percentage variation in the work function of $\%\Phi$, the structure corresponding to O_{41}/Si-CNT has the highest value of %0.44 by increasing the conduction electrons.

The recovery time (adsorption time) is one of the important parameters used for both gas sensors and drug delivery systems, which predicts the amount of time required for drug adsorption from the adsorbent, as it is highly related to the adsorption energy, and it is known that a high adsorption reaction needs a high adsorption time and vice versa.

The recovery time is calculated by the equation: [33]

$$\tau = \frac{1}{\upsilon} Exp\left(\frac{-E_{ads}}{kT}\right) \tag{12}$$

Where T, k, and υ are the temperature, Boltzmann's constant and the attempted frequency, respectively. (k$\sim 2 \times 10^{-3}$ kcal/mol K).

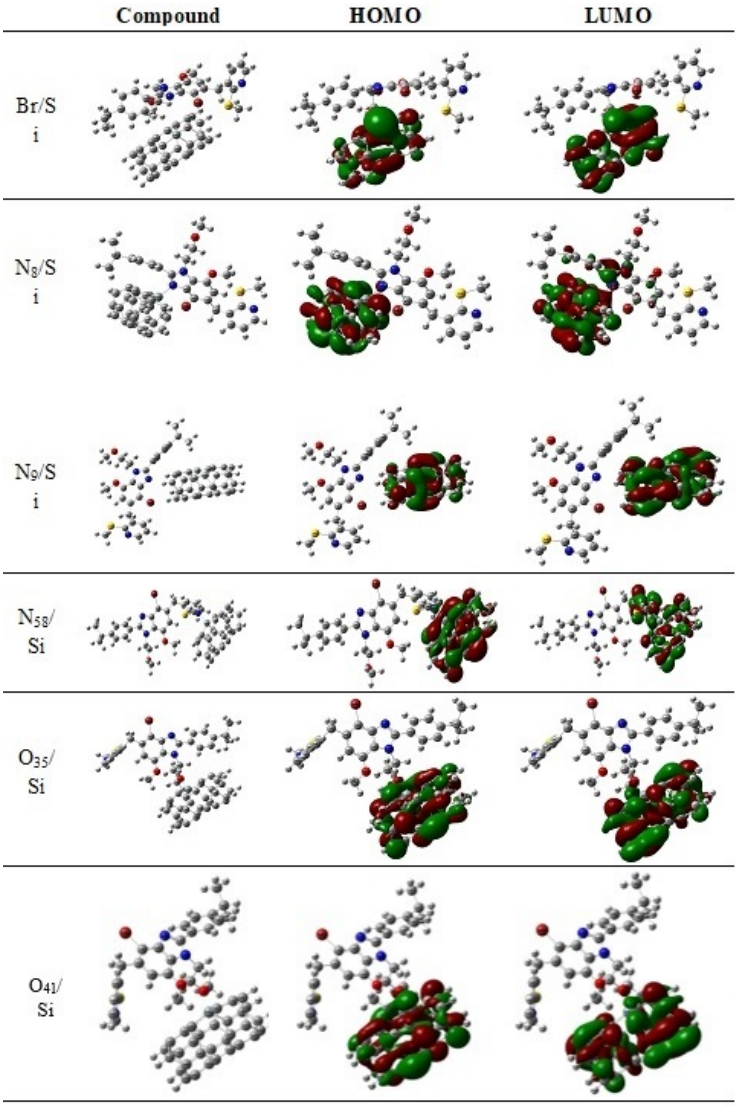

FIGURE 7. *The Frontier molecular orbital (HOMO and LUMO) of all investigated new complexes using 6-31**basis set with B3LYP-B97D level of theory; the considered iso value is 0.02 electron/bohr3.*

As the BMSF-BENZ molecule seems to be adsorbed on the Si-CNT nanotube with maximum adsorption energy, a different recovery time (Table 1) was obtained in vacuum UV- light conditions with frequencies of 3×10^{16} $\sec^{-1}$ at room temperature.

When the adsorption energy is more than 1 eV (23.061 kcal/mol) (in magnitude), a strong chemical interaction between adsorbate and adsorbent is considered to occur, and the adsorption process is then levelled as chemisorption. Therefore, the more negative value of the adsorption energy, the stronger the connection of the system and represents a higher static system, so the adsorption process between drug molecules and the adsorbent is supposed to give negative values of adsorption energy.

It is also known that in drug delivery systems, the adsorbent must have a strong interaction with the drug, and for drug sensors, there must be less energy expenditure [33].

By combining the corresponding recovery time values of those complexes in Table 1 with the percentage variation of work function given in Table 3, it has been evaluated that those complexes cannot be used as amperometric drug sensor applications of BMSF-BENZ drug molecule on Si-CNT nanotube.

Those values indicate that the adsorption process of O_{35}/Si-CNT and S/Si-CNT complexes are in physisorption nature with the desorption time values of 4.49×10^{-05}sec, and 3.33×10^{-17} sec, respectively. Among them, the complex of N_8/Si-CNT, and O_{35}/Si-CNT can be extended as a drug delivery system with a reasonable recovery time.

In order to prove the importance of (DOS) calculations in the field of quantum chemistry, researchers interested in this topic have found gradual relationships between the absorption energies between different adsorbents on the surfaces of nanoparticles and the scaling relationships between adsorption energies and interaction transfer barriers that lead to the so-called volcanic activity cut-off. These schemes indicate that the optimal catalyst must have a strong bonding with the molecules and atoms participating in the interaction, which enables these molecules to bond well on the surface of the nanoparticles, as it does not reduce or impede the absorption of products [34]. The lower E_g values indicate higher electrical conductivity, reactivity, and sensitivity. Therefore, decreased the E_g through adsorption of BMSF-BENZ drug indicates the CNT can detect the drug.

The density of states (DOS) diagram of the complex structure of the N_{58} atom of the BMSF-BENZ interacting with Si-CNT was selected to plot in Figure 7 because of the significant $\%\Delta E_g$ values are given in Table 3, each was also calculated in order to better understand the stability of the system. The change in E_g by DOS analysis can be confirmed as shown in Figure 7 by the MULTIWFN program.

It is clear in Figure 8 that the bandgap of the complex is getting narrow concerning the E_g of Si-CNT. The recovery time is related to the adsorption energy, as a high adsorption reaction needs a high adsorption time and vice versa. It is known that positive values of ΔH and G indicate that the reaction process is endothermic rather than spontaneous. In contrast, negative values of ΔH and G indicate that the reaction is an exothermic and spontaneous process [35] (see Table 4).

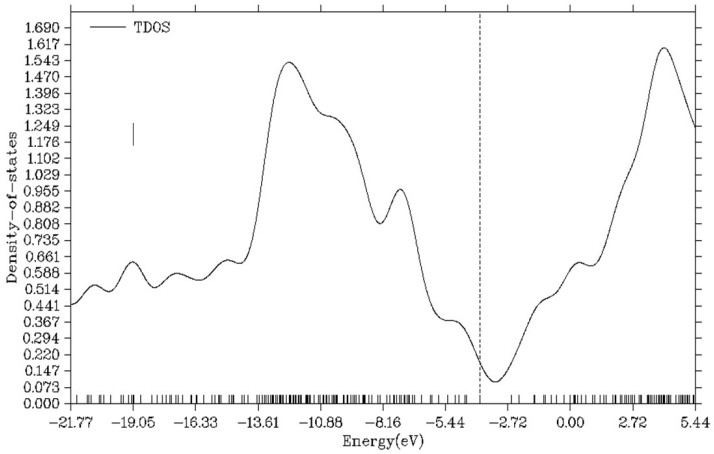

FIGURE 8. *TDOS plot for complex structure of N_{58}-BMSF-BENZ/Si-CNT. The dashed line shows the HOMO energy level.*

The obtained data for ΔH and ΔG were negative values in most of the examined complexes except upon adsorption of the drug at the bromine, oxygen, and sulfur atoms that is, these complexes are dynamically stable, and the most negative value of ΔS means the most ordered compound. Therefore, thermodynamic parameters

	Structure	ΔG	ΔH	ΔS	V_{min}	V_{max}
1	Br/Si-CNT	11.05	-0.87	15.05	-186.92	3215.99
2	N_8/Si-CNT	-19.07	-32.45	-15.07	-195.46	3224.04
3	N_9/Si-CNT	7.26	-4.32	11.26	-197.16	3205.05
4	N_{58}/Si-CNT	-14.72	-25.69	-10.72	-205.89	3216.90
5	O_{35}/Si-CNT	-7.03	-20.56	-3.03	-201.41	3214.86
6	O_{41}/Si-CNT	2.11	-4.54	6.11	-188.75	3218.96
7	S/Si-CNT	2.85	-11.83	6.85	-244.98	3208.32

TABLE 4. *Gibbs free energy (ΔG) in ($kcal.mol^{-1}$), change of enthalpy (ΔH) in ($kcal.mol^{-1}$), and change of entropy (ΔS) in (kcal/mol.K), minimum and maximum frequency in cm^{-1} for the different complexes.*

predict that the investigated complexes are more suitable and thermodynamically stable for BMSF-BENZ drug delivery.

Conclusions

In order to obtain a suitable drug delivery method for BMSF-BENZ, we examined the adsorption behaviour of BMSF-BENZ on Si-CNT surface using DFT calculations. It was observed that the BMSF-BENZ molecule was adsorbed onto the nanostructures with different adsorption energy depending on the nanotube location of the active drug atoms.

The HOMO energy (E_{HOMO}), LUMO energy (E_{LUMO}), HOMO-LUMO energy gap, and Fermi level energies were changed after the adsorption of the BMSF-BENZ drug on the surface of Si-CNT. The BMSF-BENZ drug was adsorbed on the Si-CNT nanotube with an adsorption energy of (-13.08, -43.50, -17.90, -31.29, -25.57, -16.56, and -28.05) kcal/mol in the gas phase at the B3LYP-B97D method, which is more favorable for the drug delivery system and the work function type sensor applications.

Moreover, Gibbs free energy shows that the BMSF-BENZ/Si-CNT formation exhibits spontaneous and favourable adsorption energy. Therefore, we can suggest that the Si-CNT nanotube will be a promising drug delivery medium for BMSF-BENZ drug molecules.

The QTAIM and RDG results confirm that the bond adsorption between BMSF-BENZ and Si-CNT nanotube are dominantly non-covalence or van der Walls type.

Based on the calculated results, it can be considered that the best site for adsorption of BMSF-BENZ on the Si-CNT surface is when the nanotube approaches the nitrogen atom (N_8) where the best energy and appropriate recovery time were obtained.

References

[1] C. Cooper, G. Campion, and L. J. Melton, Osteoporosis INT **2**, 285–289 (1992).

[2] S. P. Tuck and R. M. Francis, Postgrad. Med. J. **78**, 526 (2002).

[3] R. Eastell, I. T. Boyle, and et al., Int. J. Med. **91**, 71 (1998).

[4] M. Gerspacher, E. Altmann, and et al., Bioorg. Med. Chem. Lett. **20**, 5161 (2010).

[5] M. Gu, Q. Zhang, and S. Lamon, Nat. Rev. Mater. **1**, 16070 (2016).

[6] S. S. Varghese, S. Lonkar, K. K. Singh, S. Swaminathan, and A. Abdala, Sens. Actuators B Chem. **218**, 160 (2015).

[7] A. S. Rad and K. Ayub, J. Alloy. Compd. **678**, 317 (2016).

[8] P. Pannopard, P. Khongpracha, M. Probst, and J. Limtrakul, J. Mol. Graph. Model. **28**, 62 (2009).

[9] M. Conti, V. Tazzari, C. Baccini, G. Pertici, L. P. Serino, and U. De Giorgi, In Vivo **20**, 697 (2006).

[10] R. Singh and J. Lillard, Exp. Mol. Pathol. **86**, 215 (2009).

[11] R. Bakry, R. M. Vallant, and et al., Int. J. Nanomedicine **2**, 639 (2007).

[12] T. Zhang, S. Mubeen, M. V. Myung, and M. Deshusses, Nanotechnology **19**, 332001 (2008).

[13] S. M. Haidary, E. P. Córcoles, and N. K. Ali, J. Nanomater. **2012**, 1 (2012).

[14] P. A. Gowri Sankar and K. Udhayakumar, J. Nanomater. **2013**, 1 (2013).

[15] F. J. Martínez-Vázquez, M. V. Cabañas, and et al., Acta Biomaterialia **15**, 200 (2015).

[16] R. Bagheri, M. Babazadeh, E. Vessally, M. Es'haghi, and A. Bekhradnia, Inorg. Chem. Commun. **90**, 8 (2018).

[17] A. Allouche, J. Comput. Chem. **32**, 174 (2010).

[18] A. I. Alrawashdeh and J. B. Lagowski, RSC Adv. **8**, 30520 (2018).

[19] M. Athar, S. Das, P. Jha, and A. M. Jha, Supramol. Chem. **30**, 982 (2018).

[20] L. De Souza, H. Da Silva, and W. De Almedia, ChemistryOpen **7**, 902 (2018).

[21] N. Wazzan, K. Soliman, and W. Halim, J. Mol. Model. **25**, 265 (2019).

[22] M. Bilge, Anadolu University Journal of Science and Technology A - Applied Sciences and Engineering **18**, 398 (2017).

[23] A. H. Shntaif, Z. M. Rashi, Z. Al-Sawaff, and F. Kandemirli, Russ. J. Bioorg. Chem. **47**, 777 (2021).

[24] J. S. Al-Otaibi, Y. S. Mary, and et al., J. Mol. Model. **27**, 113 (2021).

[25] S. Bashiri, E. Vessally, and et al., Vacuum **136**, 156 (2017).

[26] M. A. Hossain, M. R. Hossain, and et al., Chem. Phys. Lett. **754**, 137701 (2020).

[27] J. Li, Y. Lu, and et al., Nano Letters **3**, 929 (2003).

[28] Z. Qiao, Z. Wang, C. Zhang, S. Yuan, Y. Zhu, J. Wang, and S. Wang, AIChE Journal **59**, 215 (2013).

[29] C. F. Matta and R. F. W. Bader, Proteins: Structure, Function, and Bioinformatics **52**, 360 (2003).

[30] T. Lu and F. Chen, J. Comput. Chem. **33**, 580 (2011).

[31] T. Williams and C. Kelley, Gnuplot 4.4 user manual (2011).

[32] S. U. D. Shamim, T. Hussain, and et al., J. Mol. Model. **26**, 153 (2020).

[33] Z. Al-Sawaff, S. S. Dalgic, and F. Kandemirli, Eur. J. Chem. **12**, 314 (2021).

[34] J. Aarons, L. G. Verga, N. D. M. Hine, and C. K. Skylaris, Electron. Struct. **1**, 035002 (2019).

[35] M. Shahabi and H. Raissi, J. Biomol. Struct. Dyn. **36**, 2517 (2017).